Glass Struct. Eng. (2024) 9:201–208
https://doi.org/10.1007/s40940-024-00263-2

RESEARCH PAPER

Laser-based bending of low-*E* coated flat glass: a comparative experimental study

Najoua Bolakhrif · Sandra Mee · Thomas Pauly · Adrian Baab · Tobias Rist

Received: 15 March 2024 / Accepted: 11 June 2024 / Published online: 5 July 2024

Abstract The bending of glass allows architectural freedom of design and at the same time to offer ecological and economical sustainable advantages through material-appropriate design. Coated low-emissivity and uncoated glass were treated using our innovative laser-induced bending technique. The microstructure and spectral properties of coated low-emissivity and uncoated glass were analysed by scanning electron microscopy and spectrophotometry. Due to the anisotropy of coated glass, the reflective property significantly impacts the bending process dependent on the side exposed to the laser. If the laser-based bending is focused on the uncoated side of low-emissivity glass, a faster bending process compared to the uncoated glass is observed while maintaining the same laser power. The reflective properties of low-emissivity glass are maintained after the bending process. The near infrared reflectance of low-emissivity glass remains about 50% higher than uncoated glass. This study presents the laser-based glass bending technology as fit for purpose and proves the applicability of coated bent glass for architectural purposes.

Keywords Glass · Flat glass · Coating · SEM · Glass bending · Bent glass · Low-*E* coating · Laser · Transmission · Reflection

Supplementary Information The online version contains supplementary material available at https://doi.org/10.1007/s40940-024-00263-2.

N. Bolakhrif (✉) · S. Mee · A. Baab · T. Rist
Fraunhofer Institute for Mechanics of Materials IWM, Freiburg im Breisgau, Germany
e-mail: najoua.bolakhrif@iwm.fraunhofer.de

N. Bolakhrif
GLAPE GmbH, Freiburg im Breisgau, Germany

T. Pauly
Neckargemünd, Germany

1 Introduction

In architecture, the integration of cutting-edge materials and technologies is crucial to the design of aesthetic and functional aspects of the built environment. One such key material that has made significant progress in recent years is flat glass. Transparency, i.e. the ability to transmit light, is the cornerstone of its applications in architecture and automotive. Conversely, reflectivity, i.e. the ability to reflect light back from the surface, influences its performance in reflective coatings and mirrors. In addition, absorption and scattering determine the material's efficiency in energy management and optical clarity. Traditionally limited to linear configurations, flat glass has undergone a remarkable evolution with advanced bending technologies. The applications of bent glass in architecture are diverse and range from the most iconic facades of skyscrapers to the impressive interiors of various buildings. Flat glass bending involves the controlled deformation of glass panes to achieve complex and dynamic shapes, allowing architects to push the boundaries of design while

simultaneously maintaining the structural integrity and functionality of the material. Previous research efforts have presented heat treatment methods (Finley 1999; Wang et al. 2020; Zhang et al. 2014) that ensure controlled manipulation of glass surfaces.

Windows are structural components of buildings that provide sunlight and ventilation (Fakhfakh et al. 2010). Unlike other components, glass windows constitute a weakness for the thermal integrity of buildings (Baldinelli et al. 2014). As a result, conventional windows in residential buildings are responsible for around 47% of heat loss from the building fabric (Cuce et al. 2015). A breakthrough to counteract this deficiency in glass applications in architecture and automotive is coating which is typically used for architectural and automotive glass. The need of reducing the transmittance of solar radiation (with wavelength 0.3–4 μm) has paved the way for the development of low-emissivity coated glass (low-*E* coated glass). To achieve reduced transmittance of thermal radiation, window glass is coated with metal layer of 100 nm thickness. This so-called low-*E* coating reflects near infrared radiation (approx. 700–1400 nm) while allowing visible radiation (approx. 380–700 nm) to pass through. Traditionally, the reduction of heat transmission is accomplished by increasing absorption using tinted glass, which is commonly used in the automotive sector. However, tinted glass eventually re-radiates energy at 3–50 μm, which poses this technique as unfavorable (Finley 1999). A distinction can be made between hard coating and soft coating. For hard coating, a pyrolytic tin oxide layer (emissivity $\varepsilon = 20\%$) is applied during the float glass process. The soft coating consists of several superimposed layers that are applied after the float glass process (emissivity $\varepsilon = 3\%$) (Moyer 1995). The emissivity ε describes hereby the ratio of the specific thermal radiation emitted by a body relative to an ideal body under the same temperature conditions. It was found that thin-film metallic glass coating reduces emissivity drastically, leading to superior thermal properties of coated glass (Lai et al. 2023).

Soft coating can be differentiated between coating after glass bending and coating prior to the bending process. The magnetron sputtering process allows for high-performance silver-based multilayer coating and is more efficient in reducing solar radiation transmission. Due to long cycle times and complications during the procedure, coating glass after the bending process is pricey and not applicable for industrial use cases (Finley 1999).

This research article seeks to explore the possibilities of bending low-*E* coated glass by an innovative laser-based bending technology. The technological intricacies are explained and the profound impact on architectural aesthetics and functionality is demonstrated. Technological innovation such as laser-based bending of glass can contribute to sustainability in architecture through its application with coated glass.

2 Materials and methods

Flat glass was purchased from the company caleoglas Süd GmbH. Soft coated low-*E* soda lime *float* glass is called PLANITHERM XN. Uncoated soda lime float glass is called PLANICLEAR, with a relatively low proportion of iron oxide. The glass panes have a format of 300 mm × 250 mm and a thickness of 4 mm. Each of the following experiments was conducted at least in triplicate in independent experiments that showed high reproducibility without outliers.

2.1 Laser-induced glass bending

After cleaning the glass panes, they were placed in a furnace at 570 °C. Each furnace process contained both uncoated and low-*E* coated glass to ensure comparability of the bending process. The glass was placed on a mold installed in the furnace with half of the glass panes hanging freely. An integrated CO_2 laser (10.6 μm) was used to apply a linear pattern to induce localized heating and trigger bending process. As soon as one of the glasses reached a bending of 90°, the laser program was stopped. The glass panes were used for subsequent analyses after a cooling time of approximately ten minutes. The tin bath side of the uncoated and coated glass was exposed to the laser. As a result, the low-*E* coating was directed downwards towards the laser. In total, the heat treatment lasted for about 20 min, with 2 min involving the laser process, about 8 min for preheating, and 10 min cooling phase. The temperature was measured during the bending process using a thermal camera and several thermocouples in the furnace. The thermal camera also enabled visual monitoring of the bending process.

2.2 Spectral analysis

Transmission and reflection were measured using the Tec5 AG MultiSpec Desktop/USB Unit. This system is designed for spectral measurements, allowing to analyze samples across a wide range of wavelengths. The light source was connected to the detector by glass fibers. Spectra were recorded from 185 to 1025 nm with a step width of 0.1 nm. Cycle time was set to 0.1 s and 10 cycles were measured for each spectrum. The average of 10 scans was recorded. Integration time was set to 1000 ms. The reflection and transmission of coated glass was measured on both sides, with uncoated glass as reference.

2.3 Scanning electron microscopy

To analyze the surface topography of low-*E* coated and uncoated glass before and after the heat treatment and bending process, scanning electron microscope (SEM) was applied. Using Zeiss Supra SEM in combination with an Energy dispersive X-ray spectroscopy (EDX) detector, microstructures were examined. Chemical elements were analyzed, to get further information about the composition of glass and low-*E* coating.

The glass panes were cut into 2 cm × 2 cm samples from the curved and flat areas. The samples were then sonicated in an ethanol bath for 3 s and then rinsed with ethanol. A LEICA EM ACE 200 was then used to sputter carbon onto the samples using a double-twisted carbon filament (Contents 2022). The thickness of about 5 nm was achieved by 15 to 20 pulses. The conductive layer is necessary to prevent the surface from becoming charged when the electron beam hits the sample which would distort the image and lead to the loss of structural details. The acceleration voltage, working distance and the possible detectors (backscattered electron (BSE), secondary electron (SE) or inlens) are documented in the legend of each image. For the chemical composition, using an EDAX system, a working distance of approximately 8.5 mm, a voltage of 20 kV and mainly the SE detector was used. Genesis Imaging/Mapping software, version 6.51 was used for EDAX analysis.

3 Results

3.1 Laser-induced glass bending

The target geometry corresponds to a basic bend with an outer radius of 10 mm. The 90° bending was achieved faster for low-*E* coated glass with the coated side opposing the laser than for uncoated glass with the same energy expenditure. The laser program was stopped as soon as the final geometry of the coated glass panes was reached. All parameter settings resulted in a blurred discoloration at the bend of the low-*E* coated glass panes (see Fig. 1). The glass thickness of the flat and curved area was measured for the uncoated and coated glass panes after bending. The average thickness of uncoated glass for the flat area was 3.95 mm, while the curved area showed a thickness of 3.63 mm on average. Similar results were determined for the coated glass panes (3.9 and 3.58 mm respectively). Low stresses in the curved area were found for both uncoated and coated glass (Supplementary Fig. 1). Higher stresses were found in the flat bracket area. Therefore, the cooling process may be improved to minimize these stresses.

3.2 Spectral measurement

The transmission and reflection of both, the uncoated and coated glass panes were determined before and after the heating process and laser-induced glass bending on the flat areas. For the low-*E* coated glass panes, it was observed that the coated surface facing or opposing the light source had no significant impact on transmission data and minor impact on reflection data (data not shown). For simplicity, data shown here only features coated glass with the coated surface facing the light source.

A higher transmission of solar infrared light was observed for uncoated glass compared to low-*E* coated glass, both before and after the bending process (see Fig. 2). Consequently, an approximately 50% higher reflection of infrared light was measured for low-*E* coated glass compared to uncoated glass. An impact of the bending process on the low-*E* coated glass was observed for both transmission and reflection. Transmission of infrared light of low-*E* coated glass was reduced by approximately 4%, while reflection decreased by approximately 40% as a result of the

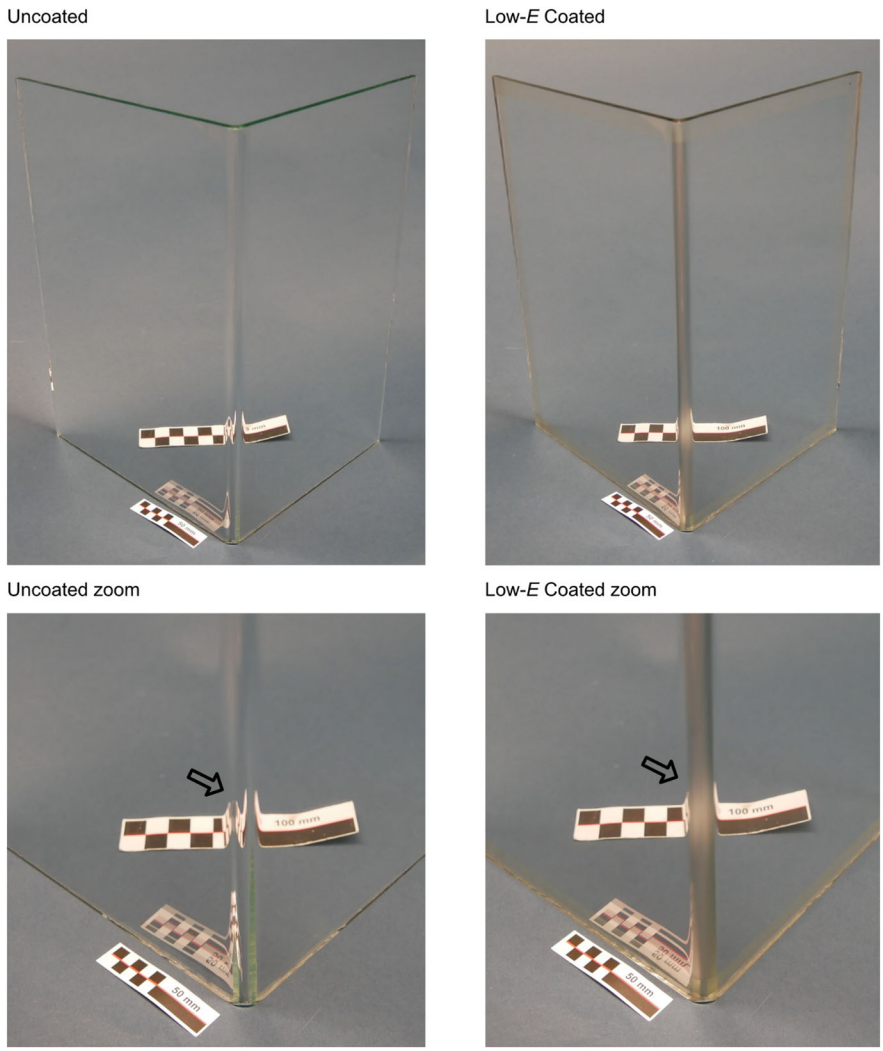

Fig. 1 Qualitative comparison after heat treatment and laser-induced bending of uncoated and low-*E* coated glass. Arrows indicate where laser lines were applied

bending process. Uncoated glass had consistent transmission but a decrease of approximately 30% in reflection of infrared light after the bending process.

3.3 Scanning electron microscopy

Before heat treatment and laser-induced bending, neither the low-*E* coated nor the uncoated glass panes showed any structural anomalies on the surface, but homogeneous, smooth topology (Fig. 3).

SEM analyses showed a change of surface topology in the curved area after heat treatment and laser-induced bending of low-*E* coated glass (Fig. 4). The surface formed furrows that are between 1.3 and 1.6 µm deep (Fig. 4, red frame), while no change in the surface was observed in uncoated glass after heat treatment and bending (Fig. 5), indicating that this furrow formation is attributable to the coating. Images of the flat surfaces show no alteration in the uncoated glass up to 10 µm (Fig. 5a). The curved area of the uncoated glass remained unchanged (Fig. 5b). However, the flat area of the low-*E* coated glass after heat treatment shows changes in the form of amorphous structures with a diameter of approximately 20 µm. These anomalies undergo a structural transformation as they approach

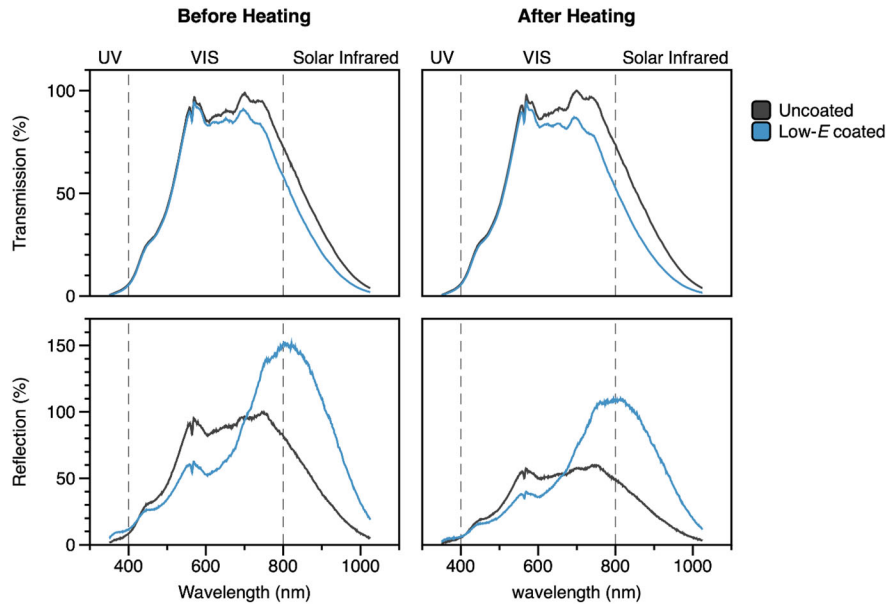

Fig. 2 Reflection and Transmission of low-*E* coated and uncoated glass panes before and after heat treatment. Blue spectra represent low-*E* coated glass, grey spectra represent uncoated glass. X-axis represents the wavelength in nm. Y-axis represents the normalized reflection and transmission relative to uncoated glass. The difference in transmission and reflection is visible in the solar infrared region

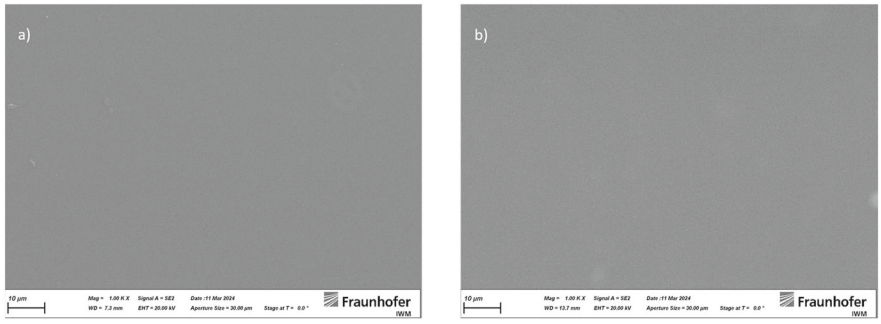

Fig. 3 SEM image of **a** uncoated and **b** low-*E* coated glass before heat-treatment and laser-induced bending. **a** Tin bath surface is facing the detector. **b** low-*E* coating is facing the detector

the curve until they eventually turn into the convolutions in the curve (Fig. 4, first column).

EDX analyses show the chemical composition of uncoated and low-*E* coated glass before and after heat-treatment (Tab. 1). In general, the low-*E* coated glass has a higher elemental composition of materials on the micrometer scale. Typical for low-*E* coatings are the elements tin (Sn) and silver (Ag), which are both represented in the coated glass before and after heating. Furthermore, titanium (Ti) was found for this type of low-*E* coating. Interestingly, the amorphous structures (Fig. 4) do not show similarities to the low-*E* coating. Here, we could detect the same elements for uncoated glass (Table 1).

The heat-treatment does not influence the elemental composition for uncoated glass, meaning that oxygen (O), silicium (Si), sodium (Na), calcium (Ca) are equally detectable for uncoated glass before and after heating. It should be noted that the tin bath side of the uncoated glass was facing the detector, whereas the tin bath side of the coated glass was not, but the coated surface was facing the detector.

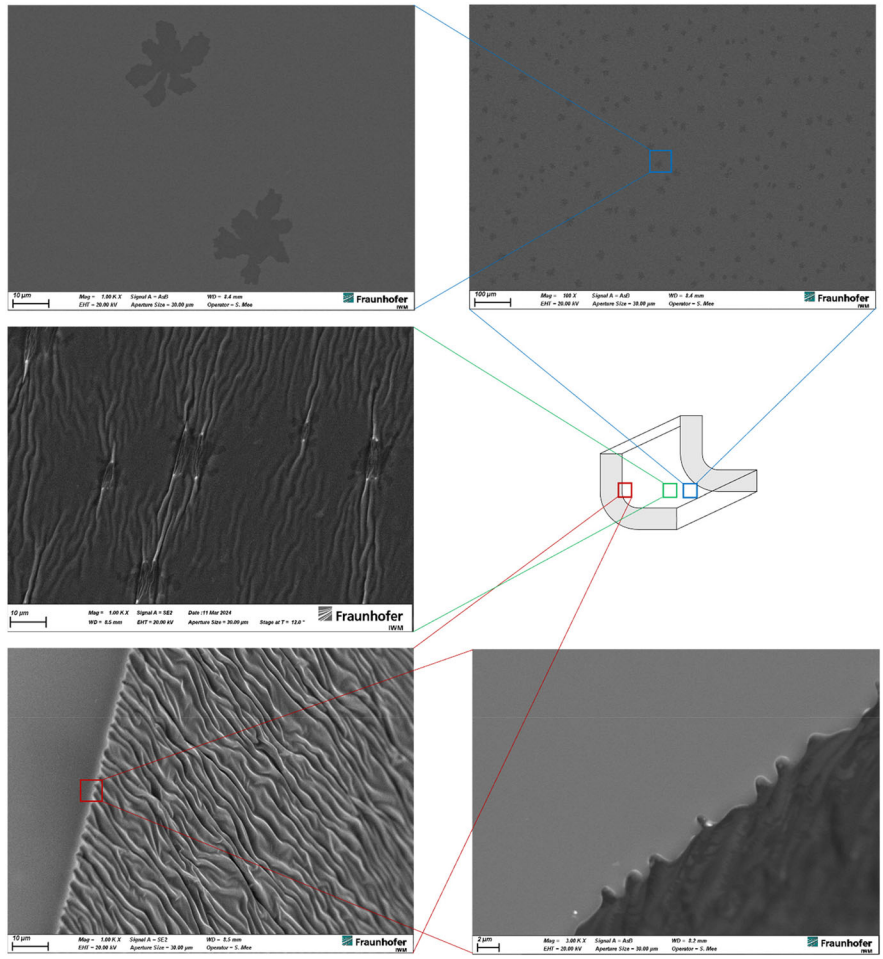

Fig. 4 SEM images of low-*E* coated glass after heat treatment and laser-induced bending. Images were taken from the flat surface (blue), curved area (green) and the cross section of the curved area (red)

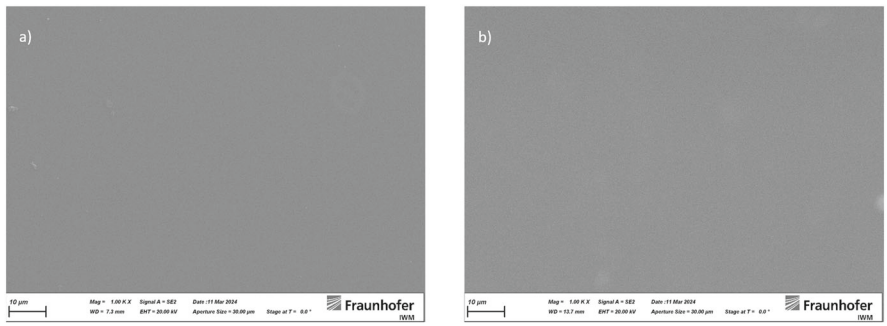

Fig. 5 SEM image of uncoated glass after heat-treatment and laser-induced bending in a) flat area, b) curved area. Tin bath surface is facing the detector

Table 1 Chemical composition determined by EDX analyses of low-*E* coated and uncoated glass samples before and after heat-treatment

Elements	Low-*E* coated before heat-treatment	Low-*E* coated after heat-treatment	Low-*E* coated Amorphous structures	Uncoated before heat-treatment	Uncoated after heat-treatment
O	x	x	x	x	x
Si	x	x	x	x	x
Na	x	x	x	x	x
Ca	x	x	x	x	x
Sn	x	x		x	x
Al		(x)			
Ag	x	x			
Mg	x	x	x	x	x
Ti	x	(x)			
Au		x			
Zn		x			

Elements in brackets show trace elements

4 Discussion and conclusion

The laser-induced bending technology is applicable for low-*E* coated glass. Low-*E* coated glass was observed to undergo an accelerated bending process using the laser-based technique while the coating is opposing the laser. A decrease in glass thickness due to material distortion was measured for the curved area of uncoated and low-*E* coated glass. However, it is reasonable to assume that the overall bending in the glass panes leads to increased structural stiffening. Consequently, the decreased thickness could be partially compensated by an increased bending resistance and lower vibration tendency. It should be noted that glass technology is in need of new methodologies to measure the stiffness and stability of complex curved glass structures.

Compared to uncoated glass, a blurred discoloration is visible in the curved area of low-*E* coated glass. Mechanical forces or the high temperatures in the furnace and during the laser-process might be potential stress factors responsible for the observed blurring. To further investigate this phenomenon, glass panes (duplicates) were treated as described in the laser-induced glass bending only with a different construction that prevented the bending (Supplementary Fig. 2). With this set-up it is possible to observe the effects of the heat and laser treatment only. Indeed, the formation of the above-mentioned amorphous structures appeared in the laser area, which let us come to the conclusion that these structures can be ascribed to high temperatures and not mechanical stress due to the bending process. Microstructural analysis by SEM shows irregular convolutions due to the compression of the low-*E* coating. These convolutions could explain the visible discoloration in the curved area. The number of convolutions decreased with increasing distance to the curved area. Amorphous structures were observed on the flat area. Similar anomalies were described in 1970 by Elmer and colleagues as phase separation on the surface of different types of glass as a result of heat treatment (Elmer et al. 1970). Although the heat treatment applied in the present study does not exceed 570 °C on the flat surfaces, similar microstructures are visible on the surface topology of the low-*E* coated glass, which could also be attributed to phase separation. Comparing these results with uncoated glass before and after the bending process, no changes were observed on the surface of the uncoated panes. These results indicate that convolution and phase separation only occur for coated glass. Comparing these results to EDX analyses, it is conceivable that these abnormal, amorphous structures are areas in which no coating is present. We assume that the high temperatures in the laser area due to the laser energy led to partial dissociation of the coating.

This irregular change in the surface topology could explain the reduced transmission and reflection of solar

infrared light of low-*E* coated glass. However, the reflective properties of low-*E* coated glass after the bending process remain superior to those of uncoated glass. In summary, the set-up, which involves the precise laser processing of flat glass in a furnace, enables flat glass to be bent. For coated glass, this technology can also be used when the uncoated side is facing the laser. In this case, the geometric properties are similar to those of uncoated glass. Although there is a slight reduction in the transmission and reflection properties of the coating, it proves the applicability for coated bent glass and high energy efficiency in architectural applications.

Our innovative laser-induced glass bending technology was demonstrated as fit for purpose to process low-*E* coated glass. This application enables glass bending of low-*E* coated glass for architectural and automotive applications, while maintaining the advantageous thermal properties of low-*E* coated glass and optical high quality of flat glass.

Acknowledgements The authors acknowledge the photographic skills of Matthias Quast and Helena Czakert for support in the revision process. Part of this work was supported by the project DiMAT. DiMAT has received funding from the European Union´s Horizon Europe research and innovation program under the Grant Agreement 101091496. Views and opinions expressed are however those of the author(s) only and do not necessarily reflect those of the European Health and Digital Executive Agency. Neither the European Union nor the granting authority can be held responsible for them.

Funding Open Access funding enabled and organized by Projekt DEAL.

Declarations

Conflict of interest On behalf of all authors, the corresponding author states that there is no conflict of interest.

References

Baldinelli, G., Asdrubali, F., Baldassarri, C., Bianchi, F., D'Alessandro, F., Schiavoni, S., Basilicata, C.: Energy and environmental performance optimization of a wooden window: a holistic approach. Energy Build. **79**, 114–131 (2014). https://doi.org/10.1016/J.ENBUILD.2014.05.010

Contents, T.O.F.: Guideline for the scanning electron microscopy and energy dispersive spectroscopy of glass samples in forensic science, pp. 1–8 (2022)

Cuce, E., Young, C.H., Riffat, S.B.: Thermal performance investigation of heat insulation solar glass: a comparative experimental study. Energy Build. **86**, 595–600 (2015). https://doi.org/10.1016/j.enbuild.2014.10.063

Elmer, T.H., Nordberg, M.E., Carrier, G.B., Korda, E.J.: Phase separation in borosilicate glasses as seen by electron microscopy and scanning electron microscopy. J. Am. Ceram. Soc. **53**(4), 171–175 (1970). https://doi.org/10.1111/j.1151-2916.1970.tb12064.x

Fakhfakh, S., Jbara, O., Rondot, S., Hadjadj, A., Patat, J.M., Fakhfakh, Z.: Analysis of electrical charging and discharging kinetics of different glasses under electron irradiation in a scanning electron microscope. J. Appl. Phys. (2010). https://doi.org/10.1063/1.3499692

Finley, J.J.: Heat treatment and bending of low-E glass. Thin Solid Films **351**(1–2), 264–273 (1999). https://doi.org/10.1016/S0040-6090(99)00087-5

Lai, C.C., Hsiao, T.C., Wang, W.H., Chang, S.W., Chen, H.L.: Emissivity and optical properties of thin-film metallic glass in the thermal infrared region. Adv. Opt. Mater. (2023). https://doi.org/10.1002/ADOM.202301517

Moyer, K.L.: Analytical and empirical evaluation of the impact of solar control glazing on the thermal environment in vans. SAE Tech. Pap. (1995). https://doi.org/10.4271/950052

Wang, Y.C., Liu, P.J., Luo, G.P., Liu, Z., Cao, P.F.: Optimization of heat treatment of glass-ceramics made from blast furnace slag. High Temp. Mater. Process. **39**(1), 539–544 (2020). https://doi.org/10.1515/htmp-2020-0059

Zhang, P., Li, X., Yang, J., Xu, S.: Effect of heat treatment on the microstructure and properties of lithium disilicate glass-ceramics. J. Non Cryst. Solidscryst. Solids **402**, 101–105 (2014). https://doi.org/10.1016/j.jnoncrysol.2014.05.023